ELSEVIER

Alzheimer's & Dementia ■ (2013) 1–12

Alzheimer's & Dementia

The effect of amyloid β on cognitive decline is modulated by neural integrity in cognitively normal elderly

Miranka Wirth[a,*], Hwamee Oh[a], Elizabeth C. Mormino[a], Candace Markley[a], Susan M. Landau[a,b], William J. Jagust[a,b]

[a]*Helen Wills Neuroscience Institute, University of California, Berkeley, CA, USA*
[b]*Life Sciences Division, Lawrence Berkeley National Laboratory, Berkeley, CA, USA*

Abstract

Objective: Alzheimer's disease (AD) pathology of amyloid β (Aβ) accumulation and neurodegeneration may be relevant to preclinical cognitive decline. The objective of this study was to relate AD-sensitive biomarkers of Aβ and neurodegeneration and their interaction to longitudinal cognitive change in cognitively normal elderly.

Methods: Thirty-eight older people completed at least three consecutive neuropsychological examinations. Using positron emission tomography (PET), Aβ plaque burden was measured with [^{11}C] Pittsburgh compound B (PiB). PiB retention was dichotomized into a positive (n = 13) and negative (n = 25) PiB status. Neurodegenerative biomarkers were extracted within AD-vulnerable regions of interest (ROIs)—namely, the hippocampus and temporoparietal cortical areas. Within each ROI, metabolism was quantified with [^{18}F] fluorodeoxyglucose (FDG) PET, and the gray matter structure was evaluated using volume (hippocampus) or thickness (cortical regions). ROI-specific functional and structural biomarkers were combined further into cross-modality neurodegenerative composite measures. Using hierarchical regression models, PiB and the neurodegenerative biomarkers were related to cognitive trajectories.

Results: PiB positivity was associated with memory and nonmemory worsening. The neurodegenerative biomarkers modified these relationships. Longitudinal cognitive decline was accelerated in those individuals who exhibited both PiB positivity and lower neurodegenerative biomarker scores, although the two measures appeared to be independent. PiB retention interacted predominantly with the cortical neurodegenerative composite for nonmemory change. Memory decline was best explained by the interaction between PiB and the hippocampal neurodegenerative composite, suggesting regional specificity of the neurodegenerative modulations.

Conclusions: Our findings indicate that cognitive trajectories deteriorate at a faster rate in cognitively normal individuals expressing Aβ burden and neurodegeneration within specific AD-sensitive regions.

Keywords: Alzheimer's disease; Cognitive aging; Memory; Preclinical decline; Amyloid; PiB; Glucose metabolism; FDG; Gray matter structure

1. Introduction

There is a need to characterize Alzheimer's disease (AD) at early stages to delay or prevent its onset. Biomarkers of AD pathology arise decades before the manifestation of the clinical syndrome [1,2]. During the preclinical phase, a pathological cascade of amyloid β (Aβ) peptide accumulation and neural injury may trigger subtle cognitive decline in cognitively normal older people [2].

Susan Landau serves as a consultant with Janssen AI. William Jagust has served as a consultant for Genentech, GE Healthcare, Bayer Healthcare, Synarc, Janssen Alzheimer Immunotherapy, TauRx, and Merck & Co. He receives research support from the National Institutes of Health.

*Corresponding author. Tel.: +510-643-6616; Fax: +510-642-3192.
E-mail address: miranka.wirth@gmail.com

1552-5260/$ - see front matter © 2013 The Alzheimer's Association. All rights reserved.
http://dx.doi.org/10.1016/j.jalz.2012.10.012

Ten percent to 30% of normal elderly exhibit fibrillar Aβ plaques [3,4], as detected in vivo with [^{11}C]-labeled Pittsburgh compound B (PiB) positron emission tomography (PET) [5]. For cognitively intact individuals with greater PiB retention, longitudinal and selected cross-sectional studies have documented cognitive decline [6–10] and greater risk of AD conversion [11,12], whereas other cross-sectional approaches have failed to show such effects [13,14].

Only a few studies to date have evaluated AD biomarkers of Aβ pathology and neuronal atrophy in the same sample. Such findings indicate that both neurodegeneration (ND; evidenced by brain atrophy, hypometabolism, and alterations in tau) and Aβ burden are risk factors for preclinical cognitive decline. Specifically, these studies have demonstrated Aβ-dependent and Aβ-independent contributions of AD-sensitive regional atrophy, particularly in the hippocampus, to poorer memory performance in normal elderly individuals [6,10,15]. Another well-established neurodegenerative biomarker that is sensitive to both presence and progression of AD is lower posterior cortical glucose metabolism [16,17]. Measured with [^{18}F] fluorodeoxyglucose (FDG) PET, lower neuronal function within AD-affected regions appears to be related to global cognitive decline in cognitively intact elderly [18,19]; yet, the potential relationship of this effect to Aβ burden remains to be established.

Relationships among AD pathological processes have been proposed, even at preclinical stages of the disease [2]. According to the amyloid cascade, the concomitant presence of ND is an essential factor for effects of Aβ burden on preclinical cognitive decline [1]. One would therefore anticipate relationships of PiB uptake and neurodegenerative biomarkers to one another and to cognitive performance. Evidence for these assumptions includes studies showing that hippocampal volume mediates the effect of Aβ on memory functions in normal older people [15]. In addition, an interaction effect between cerebrospinal fluid Aβ and tau on the rate of brain atrophy [20] has been reported. Recent diagnostic criteria further support the idea that normal older individuals with both ND and Aβ represent a more advanced stage of preclinical AD [2].

The current study examined effects of Aβ plaque burden and measures of ND within AD-sensitive regions on longitudinal memory and nonmemory change in 38 cognitively normal older adults. We hypothesized that combined evidence of (*i*) abnormal Aβ deposition (measured with PiB PET) and (*ii*) ND within the hippocampus (measured with hippocampal volume and glucose metabolism using FDG PET) and the posterior cortex (measured with cortical thickness and FDG PET) would be associated with preclinical cognitive decline. This approach allowed us to investigate interactions between ND and Aβ deposition, and the differential effects of hippocampal and posterior cortical ND on memory and nonmemory cognitive functions.

2. Methods

2.1. Study participants

A total of 38 cognitively normal elderly of the Berkeley Aging Cohort (BAC) were included in the current study. Inclusion criteria were Geriatric Depression Scale [e1] score $\leq$ 10 points, Mini Mental State Examination (MMSE) [e2] score $\geq$ 25 points, age between 60 years and 85 years, no current neurological and psychiatric disorders, no clinical diagnosis of dementia or predementia, and normal memory performance (all scores ≥ -1.5 standard deviations [SD] on the California Verbal Learning Test, Long-Delay Cued Recall [e3], and the Visual Reproduction Test, Delayed Recall and Recognition [e4], as defined using a larger group of normal older subjects).

Subjects underwent at least three consecutive neuropsychological test sessions (NTSs) with an average interval of 1.6 years (SD, 0.5 years). During each visit, the participants were examined using a 4-hour standardized NTS. The magnet resonance imaging (MRI) and PET (FDG and PiB) measurements were usually performed in two separate visits (with either MRI or PET measurements at each visit) (Table 1). Written informed consent was obtained from each participant in accordance with the institutional review boards of the University of California at Berkeley and Lawrence Berkeley National Laboratory (LBNL).

2.2. Neuropsychological data

Given the small sample, care was taken to reduce the longitudinal noise in the cognitive data by combining domain-sensitive cognitive tests into declarative memory and nonmemory (mostly executive) composite measures. The test selection procedure was based on conceptual relevance and suitable test characteristics that were adapted from the literature [21] and included minimum data loss, no ceiling/floor effects, and no minimum test scores for any subject at first and second follow-up NTS.

The memory composite was constructed from declarative memory tests (i.e., the Logical Memory Recall of Story A and Story B [e4]), Category Fluency (i.e., total count of correctly produced vegetables and animals), as well as the Visual Reproduction Test, Delayed Recall and Recognition [e4]. Episodic and semantic memory measures were combined because both appear to rely on the integrity of temporal regions [22]. Consistent with the presence of neurofibrillary tangles in temporal areas early during the course of disease [23], both cognitive markers were shown to be sensitive to preclinical changes in AD [24,25]. The nonmemory composite measure was calculated from the Stroop Test Total Correct (i.e., correct naming of printed colors) [e5], the Controlled Oral Word Association Test [e6], the Trail Making Test Part A [e7], and Digit Symbol Coding [26].

Cognitive tests were combined using the average of z scores for each subject, each measurement point and

Table 1
Sample characteristics of [^{11}C]Pittsburgh compound B (PiB)+ and PiB−individuals

Characteristic	PiB−	PiB+
Demographics		
Subjects, n	25	13
Age at first NTS, years*	74.2 (7.0), 62–87	71.5 (6.9), 61–82
Women, n (%)	14 (56)	10 (77)
Years of education	17.6 (2.1), 12–20	16.3 (2.1), 12–20
Tests and questionnaires		
MMSE score at first NTS, points	29.2 (1.1), 26–30	29.4 (0.8), 28–30
Subjects with MMSE score <28, n	3	0
Slope of MMSE scores	−0.02 (0.44)	−0.14 (0.37)
Motor speed at first NTS, tap/second, left hand	5.2 (0.7)	5.1 (0.5)
GDS score at first NTS, points	3.6 (2.9)	3.8 (2.8)
Biomarkers		
Median PiB DVR	1.04 (0.03)	1.11 (0.21)†
APOE ε4 carrier, n (%)	4 (16)	5 (38)
Measurements		
Interval, first NTS to last NTS, years	3.8 (1.2), 1.9–5.9	3.9 (1.4), 2.0–5.9
Interval, consecutive NTS, years	1.5 (0.5), 0.9–2.5	1.6 (0.5), 0.9–2.2
Subjects with a maximum of 3, 4, or 5 NTS, respectively, n	15, 7, 3	8, 5, 0
Interval, first NTS to FDG/PiB, years	1.4 (1.4), 0.02–5.3	1.7 (1.4), 0.2–3.4
Interval, FDG/PiB to MRI, years	0.2 (0.5), −0.1–1.7‡	0.2 (0.6), −0.1–1.8‡
Subjects with PET session closest to NTS 1, 2, 3, and 4, respectively, n	9, 10, 5, 1	5, 4, 4, 0
Subjects with MRI session closest to NTS 1, 2, 3, and 4, respectively, n	5, 14, 5, 1	2, 7, 4, 0
Subjects with PET/MRI sessions closest to NTS 1 or 2, n (%)	19 (76)	9 (69)

Abbreviations: NTS, neuropsychological test session; MMSE, Mini Mental State Examination; GDS, Geriatric Depression Scale; DVR, distribution volume ratio; *APOE*, apolipoprotein E; FDG, fluorodeoxyglucose; MRI, magnetic resonance imaging; PET, positron emission tomography.

NOTE. Mean and standard deviation (±) are provided, if not stated otherwise. If helpful, the range is indicated.

*Mini Mental State Examination.

†Comparison of PiB+ vs PiB−, $P \leq .01$.

‡Negative values indicate that MRI preceded PET measurements.

cognitive domain. Test-specific z scores were computed for any given measurement point using mean and SD of first-session test scores obtained from a larger cross-sectional BAC sample (n = 268 at the time of analysis; mean age, 71.1 years [SD, 9.4 years]; age range, 50–96 years; number of women, 183 [68%]; education, 17.0 years [SD, 2.2 years]; MMSE score, 28.8 points [SD, 1.6 points]).

A least-square linear regression was fitted to the composite z scores using all measurement points for each subject. The slope of the linear regression equation estimated the rate of change within each cognitive domain. The composite slopes were z-transformed using a larger longitudinal BAC sample (i.e., subjects with a minimum of three NTSs; n = 71 at the time of analysis; mean age, 72.3 years [SD 8.6 years]; age range, 56–91 years; number of women, 46 [65%]; education, 17.0 years [SD, 2.1 years]; MMSE score, 29.1 points (SD, 1.3 points]). Positive z-transformed composite slopes indicate that cognitive performance improved over time relative to the longitudinal reference sample; a negative z-transformed slope denotes cognitive decline in comparison with the longitudinal reference sample. Cross-sectional and longitudinal samples used for z score computation included the subjects of the current sample. Baseline cognitive performance was assessed using the composite z score of the NTS closest to PET measurement.

2.3. PET acquisition

The PET scanning was performed at LBNL using a Siemens ECAT EXACT HR PET scanner (Siemens, Munich, Germany).

2.3.1. PiB PET

For PiB PET scanning, approximately 15 mCi of the tracer was injected into an antecubital vein. Dynamic acquisition frames were obtained in the three-dimensional acquisition mode over 90 minutes after performing a 10-minute transmission scan (for more detail see [15]).

2.3.2. FDG PET

FDG PET scanning was performed approximately 2 hours after PiB injection. Following an injection of 6–10 mCi of the tracer, 6 × 5-minute frames of emission data were collected starting 30 minutes postinjection. All PET data were reconstructed using an ordered subset expectation maximization algorithm with weighted attenuation. Images were smoothed with a 4 × 4 × 4-mm Gaussian kernel with scatter correction.

2.4. MRI acquisition

Structural magnetic resonance (MR) images were acquired at LBNL on a 1.5-T Magnetom Avanto system (Siemens, Iselin, NJ) using a 12-channel head coil run in triple

mode. For each subject, three high-resolution T1-weighted magnetization-prepared rapid gradient echo images were collected axially with the following measurement parameters: repetition time, 2110 msec; echo time, 3.58 msec; flip angle, 15 deg; field of view, 256 × 256 mm; number of slices, 160; and voxel size, 1 × 1 × 1 mm^3.

2.5. Genotyping

The apolipoprotein E (*APOE*) genotype was determined according to standard procedures and dichotomized as an *APOE* ε4 carrier (*APOE* ε2/ε4, *APOE* ε3/ε4, and *APOE* ε4/ε4)or noncarrier. *APOE* status was not considered in the statistical analysis because of the low number of *APOE* ε4 carriers (Table 1).

2.6. PET analysis

The PiB and FDG PET data were processed using Statistical Parametric Mapping 8 (SPM8, London, UK) and FreeSurfer versions 4.5 and 5.1 (Boston, MA) software packages.

2.6.1. PiB PET

The individual PiB PET frames 6 to 34 and the summed image of frames 1 to 5 were realigned to frame 17. The realigned frames corresponding to the first 20 minutes of acquisition were averaged and coregistered to the anatomic MR image. Distribution volume ratio (DVR) images were created using Logan graphical analysis with the PiB frames corresponding to 35 to 90 minutes after injection and the gray matter masked cerebellum region as the reference tissue [e8], extracted by the automated subcortical FreeSurfer parcellation [28]. This region was chosen because it is known to be relatively unaffected by fibrillar amyloid in AD and displays comparable (nonspecific) PiB retention in AD patients and healthy control subjects in vivo [5,27].

A global PiB index was created from the averaged DVR values over frontal (cortical regions anterior to the precentral sulcus), temporal (middle and superior temporal regions), parietal (supramarginal gyrus, inferior/superior parietal lobules and precuneus), and anterior/posterior cingulate regions of interest (ROIs) demonstrated previously to exhibit greater PiB retention in AD patients compared with control subjects [27]. ROIs were extracted from the anatomic parcellation using the Desikan-Killiany atlas and the semi-automated FreeSurfer processing stream [32]. The PiB analysis was performed on native space images to minimize variance introduced by warping images to template space.

Analogous to a large body of previous studies evaluating PiB effects on cross-sectional and longitudinal cognitive markers (e.g., [6,8,14,29]), the current subjects were classified into a dichotomous high (PiB+) and low (PiB−) PiB uptake status, indicating the presence or absence of abnormal PiB retention. Using a reference sample approach, the cutoff score for PiB positivity was set to 2 SDs above the mean of the PiB index derived from an independent group of healthy young adults [14,30]. Additional post hoc analyses were carried out with the rank-transformed PiB index as an independent variable to evaluate the consistency of dichotomous PiB effects.

2.6.2. FDG PET

The six FDG PET frames were aligned to the first frame and averaged. Then, each FDG frame was realigned to the resultant mean image. The native space realigned images were summed to create one FDG scan that was then intensity normalized to the pons, expressing preserved metabolism in AD patients [31].

2.6.3. PET and MRI analysis

Biomarkers of ND included metabolic and morphological measures in brain regions targeted by AD. Brain morphology was assessed via hippocampal volume and cortical thickness; glucose metabolism was estimated via FDG PET uptake. MRI and FDG PET data processing were conducted using the native space FreeSurfer processing pipeline. The FDG PET scan was coregistered to the magnetic resonance image.

All ND biomarker measures were extracted within AD-sensitive ROIs defined by a previously published posterior cortical ROI template [16,17] and the bilateral hippocampi. The cortical ROI template comprised five AD-sensitive posterior (left and right angular, posterior cingulate, left and right temporal) regions defined in Montreal Neurological Institute space [16,17]. The template was projected onto the native space MR images and FDG scans, and the mean cortical thickness and FDG PET uptake were extracted within each ROI. ROI-wise cortical thickness and FDG values were then averaged to create a composite FDG and cortical thickness score, weighted by the number of voxels or vertices.

Hippocampal volume was measured in each hemisphere in the native space MR images using the automated FreeSurfer procedure [28] and summed across hemispheres. The hippocampal volume was adjusted for head size by removal of shared variance with total intracranial volume via regression. The mean FDG uptake in the hippocampus was obtained by mapping the hippocampal segmentation onto the native space FDG PET scan and averaging FDG values of each hemisphere using a weighted mean.

Last, for each ROI (hippocampal [H] and cortical [C] AD regions), three ND biomarker estimates were calculated: a z-transformed FDG PET uptake marker (FDG-C, FDG-H), a z-transformed structural MRI marker (MRI-C, MRI-H), and a summed cross-modality ND composite marker evaluating the combined impact of FDG PET and MRI measures for each ROI (Comp-C, Comp-H).

2.7. Data analysis

The statistical analysis procedure was based on multiple regression models. This statistical procedure was chosen because of its high flexibility and common application in the examination of moderation effects [33,34].

The data analysis was performed with the statistical software package PASW18. The significance level was set to $P \leq .05$, two tailed. Sample and measurement characteristics of PiB+ individuals and PiB− individuals were compared using χ^2 test statistics for categorical variables or independent *t* tests for continuous variables. Nonparametric tests were performed whenever normality assumptions were violated.

2.8. Interrelationships among AD biomarkers

Relationships among the biomarkers of interest were examined using linear regression models. First, the ND biomarker of interest was entered as the dependent variable, and dichotomous or continuous PiB uptake as the independent variable. Second, relationships between FDG PET uptake and structural MRI measures were assessed for the hippocampal and the cortical ROIs. Covariates were added if necessary using the procedure described next.

2.9. Relationships between AD biomarkers and cognitive performance

Multiple linear regression models were fitted to relate the biomarkers to domain-specific longitudinal cognitive change (z-transformed composite slopes) as the dependent variables of interest. Each ND biomarker of interest was entered as the independent variable (or predictor). PiB binding was treated as a dichotomous (PiB+, PiB−) or continuous variable. The three ND biomarkers were fitted separately for each ROI (hippocampus and cortical AD region) as continuous variable.

Given the current sample size, care had to be taken in selecting covariates to maintain reasonable power [35]. Because of the relatively low ranges of age and education in our sample, minimal correlations of these covariates to the dependent variables could be expected. We assessed associations of age, education, and gender in preliminary regression analyses. Only in case of a considerable association ($P < .1$) of any covariate with the dependent variable of interest were regression models rerun including the respective covariate or covariates.

The linear regression analyses were carried out using a hierarchical procedure that has been explained in detail elsewhere [34]. For each hierarchical regression model, two biomarkers (BM) of interest were entered:

$$Y = b0 + bj\ BM1 + bk\ BM2 + bi\ (BM1 \times BM2) + e\ (\text{Model A})$$

The dichotomous PiB uptake (BM1) variable was dummy coded with PiB+ = 0 and PiB− = 1, and fitted at level 1 of the regression model. The ND biomarker of interest (BM2) was entered at level 2. The interactive term of PiB and the ND biomarker of interest (BM1 × BM2) was evaluated at level 3. The regression coefficients (b) were tested for significance. Note, the interaction is determined by the product of the two biomarkers (BM1 and BM2) in the equation (Model A) and indicates moderation effects [36]. In our study, a moderation effect suggested that the effect between one BM and the outcome, Y, is altered by the given values of the other BM in the model. The hierarchical regression models were repeated for the z-transformed baseline cognitive composite measures. For reasons of simplicity, main effects of PiB uptake and the interaction between PiB and the ND biomarker of interest were evaluated on baseline cognitive performance.

In two post hoc analysis procedures, significant interactions were explored to understand their significance. Predicted cognitive (memory and nonmemory) scores were calculated for each PiB uptake group at low (−1 SD of the mean), medium (0 SD of the mean), and high (1 SD of the mean) values of the continuous ND biomarkers of interest using the unstandardized coefficients of the regression equation (Model A) [34,37]. The predicted scores were graphed and evaluated descriptively.

In addition, the simple slopes were assessed within each PiB group. The regression coefficient b_i indicates that the slopes of BM1 and BM2 differed from each other, but not whether the slope of BM2 on cognition (Y) within each PiB group (BM1) differed from zero. The PiB variable was dummy coded with PiB+ = 0 to test the significance of the regression coefficient (b_k) of each ND biomarker of interest within the PiB+ group. Dummy coding was chosen because the regression coefficient (b_k) of BM2 represents a conditional effect at the value of zero of BM1 in a regression model with an interaction [34]—here, Model A. To assess the significance of the regression coefficient (b_k) of each ND biomarker of interest within the PiB− group, the dummy-coded PiB variable was recoded in such a way that PiB− individuals received values of zero.

For each regression model, standardized residuals [35] and Cook's distance [38] were evaluated case by case to detect outliers and influential cases, respectively. A model-fit analysis assessed the change of explained variance (R^2) by means of *F* ratio statistics at each level (n) compared with the previous level (n − 1) of the hierarchical regression model. The explanatory power of the regression models within each ROI was evaluated descriptively using the explained variance (adjusted R^2) of the overall regression model (at level 3).

2.10. Exploratory analysis

In an exploratory analysis, we evaluated PiB effects on the longitudinal cognitive change for the following subcomponents: visual memory (slopes over mean z-transformed scores of Delayed Recall and Recognition tests at each measurement point), semantic memory (slopes over mean z-transformed scores of the Category Fluency test at each measurement point), logical memory (slopes over mean z-transformed scores of the Logical Memory Recall test at each measurement point), visuospatial ability (z slopes over mean z-transformed scores for Digit Symbol Coding and Trail Making Test Part A at each measurement point), and verbal executive functions (slopes over mean z-transformed

scores for the Oral Word Association Test and Stroop Test Total Correct at each measurement point).

Simple regression models were carried out with dichotomous (dummy coded, PiB+ = 1) or continuous PiB uptake as an independent predictor and the cognitive measure of interest as the dependent variable. In addition, effects of PiB uptake on memory and nonmemory decline were explored using a hierarchical regression model (Model A) with dichotomous PiB uptake, gender, and the interactive term of gender and PiB, because recent research has demonstrated cross-sectional cognitive decline selectively in PiB+ women [29].

3. Results

3.1. Sample and measurement characteristics

A threshold of 1.08 was obtained for the classification of the PiB binding status resulting in 13 PiB+ and 25 PiB− elderly subjects. As shown in Table 1, the global cortical PiB binding in the PiB+ subjects was measured with a median DVR of 1.11 (SD, 0.21). PiB status was not associated significantly with gender and age, years of education, MMSE score, Geriatric Depression Scale score, and basic motor speed as measured at first NTS.

Individuals of both PiB groups had a median of three NTSs and were monitored for about 4 years on average. PiB and FDG measurements were conducted on the same day (with the exception of a 22-day time lag for one subject) and are therefore reported collectively. For all participants, PET measures were obtained subsequent to the first NTS. There were no significant group differences in the time intervals of the PET sessions to the first NTS or MRI measurement. For the majority of individuals, the neuroimaging measurements were performed closest in time (with a maximum time lag of about 11 months) to the first or second NTS (Table 1). In detail, the following absolute time lags were measured for PET and MRI sessions to the flanking NTS: PET absolute time lag: mean, 0.4 year; SD, 0.2 year; range, 0.02–0.9 year; MRI absolute time lag: mean, 0.3 year; SD, 0.2 year; range, 0.02–0.8 year).

3.2. Interrelationships among AD biomarkers

No significant associations could be detected for PiB uptake and any of the ND biomarker estimates. For the cortical (C) AD regions, the following estimates were obtained for the dichotomous PiB predictor (for simplification, only standardized β coefficients are provided): FDG-C, $\beta = 0.13$, $P = .44$; MRI-C, $\beta = 0.13$, $P = .44$; and Comp-C, $\beta = 0.17$, $P = .30$. A similar pattern was observed for the hippocampus (H): FDG-H, $\beta = 0.20$, $P = .23$; MRI-H, $\beta = -0.14$, $P = .41$; and Comp-H, $\beta = 0.04$, $P = .80$). This observation is shown for the composite ND parameters in Fig. 1. The results did not change, when continuous PiB uptake was fitted and controlled for covariates (all P values $> .05$, data not shown). Also, there were no significant relationships between the FDG-C and the MRI-C variables or between the FDG-H and the MRI-H measures in the current sample (all P values $> .4$, data not shown).

3.3. Relationships between AD biomarkers and cognitive performance

Hierarchical regression models assessed the effect of the biomarkers on longitudinal nonmemory change as measured via regression slopes. In these models, a significant first-level effect of abnormal PiB binding status (PiB+, PiB−) was detected, indicating that PiB positivity was associated with nonmemory decline (Table 2, Fig. 2). We also observed significant interactions between PiB binding status and each cortical ND biomarker for the nonmemory trajectories (Table 2). The explanatory power (Table 2) was most prominent for Comp-C (adjusted $R^2 = 0.38$, Model 3), followed by FDG-C (adjusted $R^2 = 0.22$, Model 1) and MRI-C (adjusted $R^2 = 0.20$,

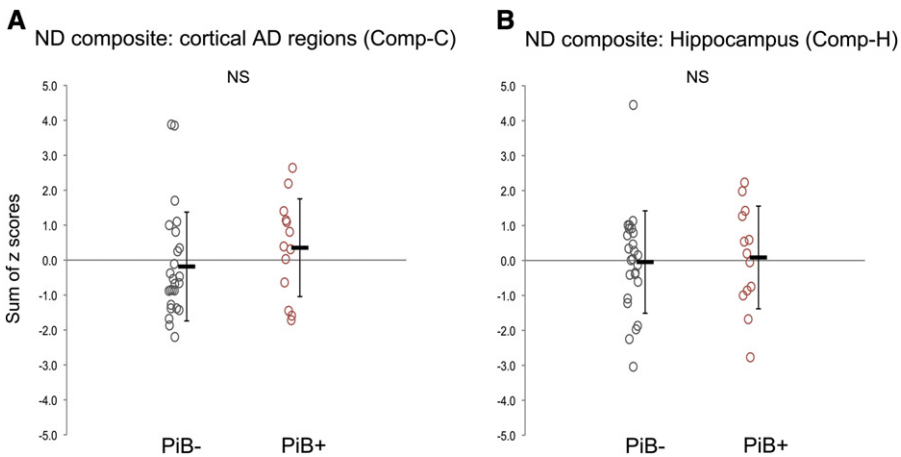

Fig. 1. (A, B) Relationships between [^{11}C]Pittsburgh compound B (PiB) uptake and the neurodegenerative biomarkers. Graphs display the neurodegenerative (ND) composite biomarkers of the cortical AD regions template (A) and the hippocampus (B) for PiB+ individuals (red circles) and PiB− individuals (black circles). Black bars indicate the group-specific means with standard deviation. There were no significant (NS) differences between the PiB groups across ND composite biomarkers. Abbreviation: AD, Alzheimer's disease.

Table 2
Hierarchical regression analysis (nonmemory); relationships between [^{11}C]Pittsburgh compound B (PiB) uptake and the neurodegenerative biomarkers to nonmemory change

Model	Variable	B value*	SE B value	β†	Zero-order correlation	ΔR^{2}‡	Adjusted R^2
Model 1: FDG-C							
Step 1	PiB§	0.48¶	0.23	0.33¶	0.33	0.11¶	0.08
Step 2	PiB	0.51¶	0.23	0.35¶		0.03	0.09
	FDG-C	0.13	0.11	0.19	0.14		
Step 3	PiB	0.53¶	0.21	0.37¶		0.14¶	0.22
	FDG-C	0.40¶	0.15	0.57¶			
	PiB × FDG-C	−0.53¶	0.21	−0.54¶			
Model 2: MRI-C							
Step 1	PiB	0.48¶	0.23	0.33¶	0.33	0.11¶	0.08
Step 2	PiB	0.49¶	0.23	0.34¶		0.01	0.07
	MRI-C	0.07	0.11	0.10	0.06		
Step 3	PiB	0.58¶	0.22	0.40¶		0.15¶	0.20
	MRI-C	0.65¶	0.25	0.92¶			
	PiB × MRI-C	−0.70¶	0.27	−0.90¶			
Model 3: Comp-C							
Step 1	PiB	0.48¶	0.23	0.33¶	0.33	0.11¶	0.08
Step 2	PiB	0.52¶	0.23	0.36¶		0.04	0.09
	Comp-C	0.09	0.07	0.19	0.13		
Step 3	PiB	0.63#	0.19	0.44#		0.28#	0.38
	Comp-C	0.48#	0.11	1.04#			
	PiB × Comp-C	−0.55#	0.14	−1.00#			

Abbreviations: SE, standard error; FDG-C, fluorodeoxyglucose (FDG) positron emission tomography (PET) uptake marker of the cortical (C) Alzheimer's disease regions; MRI-C, magnetic resonance imaging (MRI) marker of the cortical Alzheimer's disease regions; COMP-C, neurodegenerative composite marker evaluating the combined impact of FDG PET and MRI measures of the cortical region AD regions.

*Unstandardized regression coefficient.

†Standardized coefficient.

‡Change (Δ) in explained variance (R^2).

§Dummy coded: PiB+ = 0, PiB− = 1.

¶$P \leq .05$.

#$P \leq .01$.

Model 2). In the regression models, an outlier was identified. When deleting the case from the data sample, the main and interactive effects of PiB and the ND biomarkers (FDG-C and Comp-C) were increased, and the explained variance of the overall model improved for the Comp-C (adjusted $R^2 = 0.56$, Model 3) and FDG-C (adjusted $R^2 = 0.49$, Model 1) parameters.

For the hippocampal ND biomarker, there were no significant interactions with PiB uptake status on longitudinal nonmemory change (all P values $> .1$, data not shown). PiB main and interaction effects were absent in the baseline measure of nonmemory performance (all P values $> .1$, Fig. 2).

A post hoc analysis of the significant interactions indicated that the level of the cortical ND biomarker moderated the relationship between PiB uptake and nonmemory decline. Nonmemory decline was accelerated within individuals who expressed both PiB+ and lower ND biomarker values (Fig. 3A). Simple slope tests within each PiB group further indicated that the ND biomarkers were related to nonmemory decline only within PiB+ individuals (Table 2; for PiB−, all P values $> .05$; Fig. 3B).

Regression models with continuous PiB quantification confirmed significant interactions between PiB uptake and each cortical ND biomarker on nonmemory decline (all P values $< .05$, data not shown), and there was a trend for the first-level effect of PiB uptake on this outcome measure ($B = -0.02$, $SE = 0.01$, $\beta = -0.30$, $P = .06$).

Hierarchical regression models with longitudinal memory change as the dependent variable detected an effect of abnormal PiB binding status. The effect suggested that PiB positivity was related to memory decline (Table 3, Fig. 2). There were significant interactions of PiB binding status with the hippocampal ND biomarkers (FDG-H, Comp-H). The explained variance (Table 3) was greater for the regression model that included the Comp-H variable (adjusted $R^2 = 0.31$, Model 3) compared with the FDG-H variable (adjusted $R^2 = 0.26$, Model 1).

For the cortical ND biomarkers, there were no significant interactions with PiB uptake status on memory decline (all P values $> .1$, data not shown). PiB main and interactive effects were further absent for baseline memory scores (all P values $> .1$, Fig. 2).

Post hoc elaboration of the significant interactions indicated that PiB+ individuals declined fastest when expressing lower values of the FDG-H or the Comp-H parameters (Fig. 3A). The relationships between FDG-H and Comp-H to memory decline were significant only within PiB+ individuals (Table 3; for PiB−, all P values $> .05$; Fig. 3B).

PiB quantification as a continuous measure did not change the results. The analyses confirmed significant

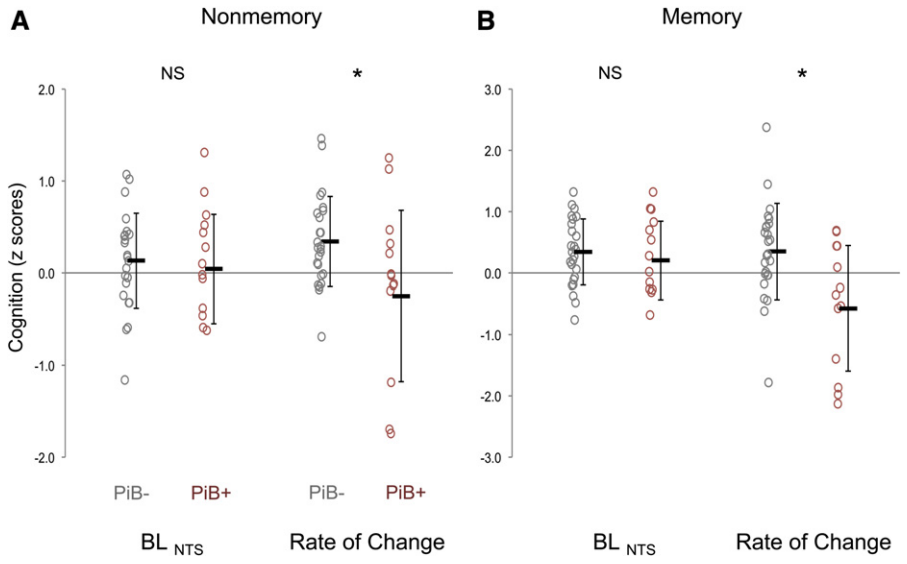

Fig. 2. (A, B) Relationships between [^{11}C]Pittsburgh compound B (PiB) uptake and cognition. Graphs show z-transformed composite cognitive scores for baseline measurements (BL_{NTS}) and the rate of change for PiB+ individuals (red circles) and PiB− individuals (black circles). Black bars indicate the group-specific means with standard deviation. PiB positivity was related significantly (asterisk) to longitudinal nonmemory (A) and memory (B) decline, but not cross-sectional baseline performance (not significant [NS]). NTS, neuropsychological test session.

interactions for FDG-H and Comp-H on memory decline (all P values $< .05$, data not shown). There was a significant first-level effect of continuous PiB on this cognitive marker ($B = -0.03$, $SE = 0.01$, $\beta = -0.34$, $P < .05$).

3.3.1. Exploratory analysis

Simple regression models were carried out to examine the main PiB effects on longitudinal cognitive change for specific cognitive subcomponents. They indicated (in part with trends) that PiB positivity (dummy-coded, PIB+ = 1) was related to decline in semantic memory ($B = -0.68$, $SE = 0.30$, $\beta = -0.36$, $P < .05$), visual memory ($B = -0.10$, $SE = 0.32$, $\beta = -0.45$, $P < .01$), and visuospatial abilities ($B = -0.47$, $SE = 0.24$, $\beta = -0.32$, $P = .05$). No significant PiB effects were observed for logical memory ($B = 0.05$, $SE = 0.37$, $\beta = 0.03$, $P = .88$) and executive functions ($B = -0.20$, $SE = 0.34$, $\beta = -0.10$, $P = .56$). When PiB uptake was evaluated as a continuous variable, we observed similar effects, except in trends for semantic memory ($B = -0.02$, $SE = 0.01$, $\beta = -0.30$, $P = .07$) and visuospatial abilities ($B = -0.02$, $SE = 0.01$, $\beta = -0.30$, $P = .07$).

There was no evidence for a potential enhancement of PiB-associated longitudinal memory and nonmemory decline among women (all P values $> .1$, data not shown).

4. Discussion

This study examined the relationship between AD biomarkers of Aβ burden and neurodegeneration to cognitive performance in cognitively normal older people. There were two key findings. First, Aβ burden was related to longitudinal but not cross-sectional cognitive decline. Second, the effect of Aβ pathology on longitudinal decline interacted with the neurodegenerative biomarkers such that in individuals with evidence of Aβ and lower neural integrity, cognitive worsening was exacerbated. These patterns were regionally specific, demonstrating dissociated relationships for memory and nonmemory cognition with hippocampal and cortical AD regions, respectively.

Higher PiB retention was associated with longitudinal cognitive decline but did not affect baseline performance. Our results mirror prior findings of adverse PiB effects on cognitive trajectories that were based on independent cohorts [7,11,12], larger sample sizes [11], and extended observation periods [6]. Our findings expand these reports by documenting that Aβ-related cognitive decline could also be detected in a smaller sample and with a relatively brief follow-up period. Furthermore, it should be noted that Aβ-related cognitive decline was present for memory and (albeit to a lesser degree) nonmemory functions, corroborating previous observations [6,12,39] that a range of cognitive abilities could be affected in cognitively normal older individuals.

In our sample there were no cross-sectional associations of PiB to baseline cognitive performance. Cross-sectional studies have often failed to demonstrate clear-cut effects of Aβ pathology on cognitive performance, using dichotomous [3,13,14,40,41] or continuous [15] PiB quantifications. Subtle cross-sectional effects of Aβ burden on cognition can be blurred by intersubject heterogeneity in cognitive abilities, insensitive cognitive measures, and mixed ND pathology or reserve factors [15,42]. Although some interindividual approaches have reported Aβ-related cognitive decline [9,10,29,39,43], intraindividual cognitive change could be a superior cognitive marker at early preclinical stages [44].

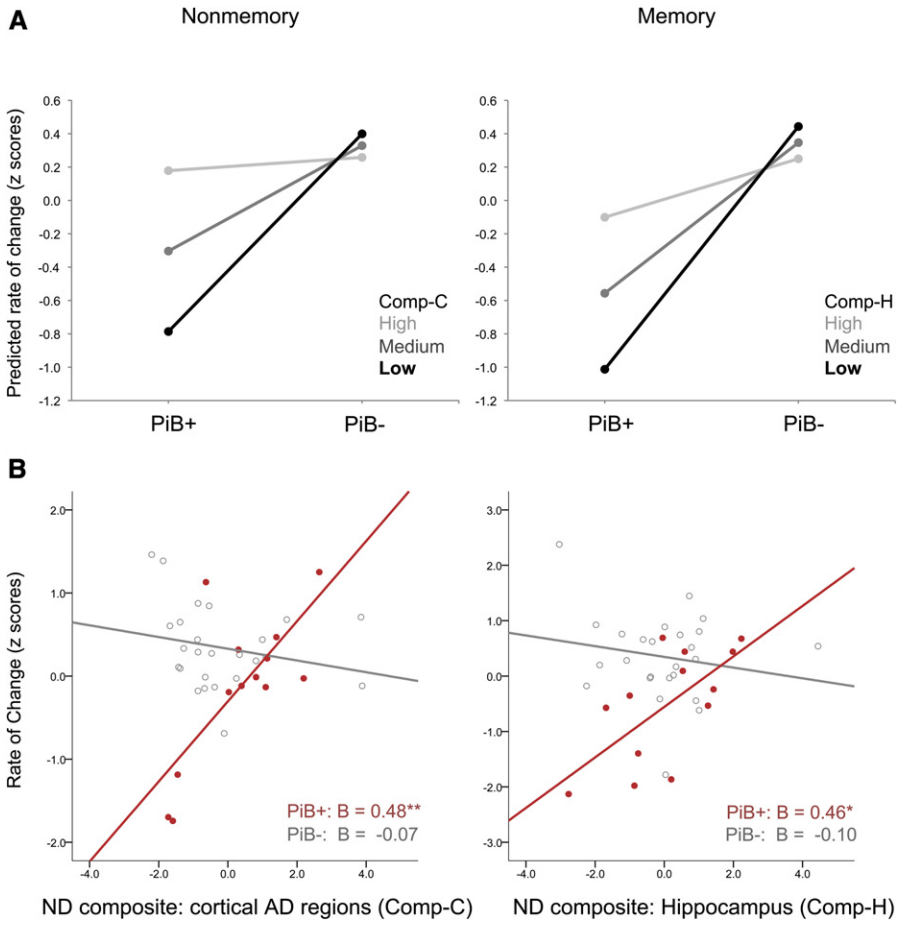

Fig. 3. Interaction between [^{11}C]Pittsburgh compound B (PiB) uptake and the composite neurodegenerative (ND) biomarker for memory and nonmemory change. (A) The graphs illustrate the relationships between PiB uptake and predicted nonmemory (left) and memory (right) change for different levels of the ND composite biomarker (low, −1 standard deviation [SD]; medium, 0 SD; and high, 1 SD). Greater PiB uptake was related to exacerbated cognitive decline for individuals with lower ND biomarker scores within specific regions—that is, the cortical AD region (Comp-C) for nonmemory and the hippocampus (Comp-H) for memory. (B) Regression plots display results of the simple slope analysis. Lower ND biomarker scores were related to nonmemory (left) and memory (right) decline, selectively (asterisks) within PiB+ individuals (red circles). Linear trends (solid lines) and unstandardized regression coefficients (B) are provided. Abbreviation: AD, Alzheimer's disease.

More important, the effect of dichotomous and continuous PiB uptake on nonmemory and memory trajectories interacted with the majority of the ND AD biomarkers. That is, in individuals with higher Aβ disposition and lower neural integrity, cognitive decline was accelerated. The findings suggest that individuals with both higher Aβ burden and signs of ND within AD-vulnerable regions fall within a more advanced preclinical stage than those with high Aβ load but without ND biomarker abnormalities. There are, however, alternative interpretations, as to why an AD-like pattern of biomarkers might occur in some cognitively normal elders.

In the amyloid cascade model, Aβ accumulation is thought to trigger ND, eventually leading to cognitive decline [1,2]. We did not find direct support for this mediatory hypothesis, because PiB and the ND biomarkers seemed to be independent, in contrast to other reports [45,46]. Specifically, not all PiB+ subjects demonstrated lower ND biomarkers values, which were also seen in the absence of Aβ, as has been reported in another normal cohort [47]. There are several possible explanations for these observations, including insensitivity of our Aβ measurement, dissimilar times of exposure to Aβ-related neurotoxicity, or the possibility that the ND biomarkers are independent from or even precede Aβ deposition in some individuals. In such a scenario, early ND could result in the requirement for greater neural activity that may lead to greater deposition of Aβ [48]. As recently proposed, these ND biomarkers could reflect non-AD pathological changes [47].

It is worth noting that the ND biomarkers moderated effects of PiB on cognitive decline in a region-dependent manner. Effects of Aβ disposition on nonmemory decline were modified by the presence of ND within the posterior cortical AD regions and within the hippocampus for memory. The observed pattern suggests that the role of neural integrity in relation to cognition is region specific. Moreover, in the current sample, there were no isolated effects of the ND biomarkers on cognitive decline. It therefore appears that, in the setting of Aβ pathology, regional reduction in structural and

Table 3
Hierarchical regression analysis (memory); relationships between [^{11}C]Pittsburgh compound B (PiB) uptake and the neurodegenerative biomarkers to memory change

Model	Variable	B value*	SE B	β†	Zero-order correlation	Δ$R^{2‡}$	Adjusted R^2
Model 1: FDG-H							
Step 1	PiB§	0.87¶	0.30	0.44¶	0.44	0.19¶	0.17
Step 2	PiB	0.93#	0.30	0.47#		0.02	0.17
	FDG-H	0.15	0.15	0.16	0.07		
Step 3	PiB	0.99#	0.29	0.50#		0.10¶	0.26
	FDG-H	0.52¶	0.21	0.54¶			
	PiB × FDG-H	−0.64¶	0.28	−0.50¶			
Model 2: MRI-H							
Step 1	PiB	0.87¶	0.30	0.44¶	0.44	0.19¶	0.17
Step 2	PiB	0.86¶	0.30	0.43¶		0.002	0.15
	MRI-H	0.04	0.15	0.04	0.10		
Step 3	PiB	0.82¶	0.30	0.41¶		0.05	0.17
	MRI-H	0.34	0.25	0.36			
	PiB × MRI-H	−0.45	0.31	−0.38			
Model 3: Comp-H							
Step 1	PiB	0.87¶	0.30	0.44¶	0.44	0.19¶	0.17
Step 2	PiB	0.89¶	0.30	0.44¶		0.02	0.16
	Comp-H	0.09	0.10	0.13	0.12		
Step 3	PiB	0.90#	0.27	0.46#		0.16¶	0.31
	Comp-H	0.46¶	0.16	0.69¶			
	PiB × Comp-H	−0.55¶	0.19	−0.68¶			

Abbreviations: SE, standard error; FDG-H, fluorodeoxyglucose (FDG) positron emission tomography (PET) uptake marker of the hippocampus (H); MRI-H, magnetic resonance imaging (MRI) marker of the hippocampus; COMP-C, neurodegenerative composite marker evaluating the combined impact of FDG PET and MRI measures for the hippocampal region.

*Unstandardized regression coefficient.

†Standardized coefficient.

‡Change (Δ) in explained variance (R^2).

§Dummy coded: PiB+ = 0, PiB− = 1.

¶$P \leq .05$.

#$P \leq .01$.

functional neural integrity becomes a critical factor for the time-dependent loss of cognitive functions, sustained by the particular brain area. These results coincide with findings showing that Aβ and tau interact to produce longitudinal regional atrophy [20] and cognitive decline [49].

Last, our analysis demonstrated that the combination of structural and functional ND biomarkers could be beneficial in defining preclinical progression. Both neuroimaging biomarkers were uncorrelated within the hippocampus and cortical regions, as might be expected in cognitively normal samples. Yet, the composite measure of FDG PET and MRI parameters within each ROI yielded the highest explanatory power for longitudinal cognitive decline. This can be explained by the fact that, multi-modal biomarker combination may reduce inherent measurement noise and allow detection of subtle ND alterations.

Our study has some limitations. First, it is characterized by a small sample size. Although our key findings converge well with the existing literature, the observed PiB and ND biomarker interactions on cognitive decline should be replicated. Recent research has further demonstrated selective effects of PiB retention on cross-sectional cognition in women [29]. The PiB groups in our study were not differentiable statistically in their gender distribution, but the number of women was somewhat higher among the PiB+ subjects. This sample attribute could have augmented the PiB effect on cognitive trajectories; however, the current analysis did not support this assumption. Last, comparable with a previous study [7], neuroimaging biomarkers were not always collected at the first NTSs, but at a variety of times during the follow-up period. We feel, however, that this was unlikely to affect the results for several reasons. For the majority (74%) of the individuals, PET and MRI measures were obtained within approximately 11 months of the first or second NTS. Existing evidence [50] further suggests slow rates of change for PiB accumulation in normal older individuals. Subjects, characterized as PiB− or PiB+, were therefore considered rather unlikely to change PiB status over the relatively brief time window of follow-up.

The current results, in the aggregate, add data to the argument that the deposition of Aβ in cognitively normal older people is a biologically significant event that coincides with cognitive worsening over time. The combination of Aβ burden with metabolic and morphological reductions within AD-sensitive regions appears to exacerbate preclinical cognitive decline. Our findings suggest that the multimodal integration of AD biomarkers is important for our understanding of preclinical cognitive decline.

Acknowledgment

This work was supported by National Institutes of Health grant AG034570 and the Swiss National Science Foundation grant PA00P1_131515. We gratefully thank the following contributors: Martina Studer (University of Bern, Switzerland, behavioral analysis), Cindee Madison (University of California [UC] at Berkeley, neuroimaging analysis), Tad Haight (UC at Berkeley, statistics support), Natalie Marchant (UC at Berkeley, manuscript editing), Bénédicte Rossi (UC at Berkeley, discussion).

RESEARCH IN CONTEXT

1. Systematic review: We searched all reports in PubMed with the terms Aβ, longitudinal, aging, and cognition. For each term, we also explored all alternative names and included relevant references from previous articles. Several reports focused on associations of amyloid or neurodegenerative Alzheimer's disease (AD) biomarkers with cross-sectional and longitudinal cognitive decline in cognitively normal older individuals. However, none of the studies assessed relationships of these biomarkers with longitudinal cognitive change in the cognitively normal elderly.
2. Interpretation: Our results substantiate observations that Aβ deposition in cognitively normal older people is related to cognitive decline. Consistent with the AD biomarker model, the combination of Aβ burden with biomarkers of neurodegeneration accelerated preclinical cognitive decline.
3. Future directions: Future studies are needed to determine factors that foster the simultaneous occurrence of amyloid and neurodegenerative biomarkers, the factors associated with neurodegeneration, and their relative contribution to cognitive decline in normal older individuals.

References

[1] Jack CR Jr, Knopman DS, Jagust WJ, Shaw LM, Aisen PS, Weiner MW, et al. Hypothetical model of dynamic biomarkers of the Alzheimer's pathological cascade. Lancet Neurol 2010; 9:119–28.
[2] Sperling RA, Aisen PS, Beckett LA, Bennett DA, Craft S, Fagan AM, et al. Toward defining the preclinical stages of Alzheimer's disease: recommendations from the National Institute on Aging–Alzheimer's Association workgroups on diagnostic guidelines for Alzheimer's disease. Alzheimers Dement 2011;7:280–92.
[3] Mintun MA, Larossa GN, Sheline YI, Dence CS, Lee SY, Mach RH, et al. [11C]PIB in a nondemented population: potential antecedent marker of Alzheimer disease. Neurology 2006;67:446–52.
[4] Quigley H, Colloby SJ, O'Brien JT. PET imaging of brain amyloid in dementia: a review. Int J Geriatr Psychiatry 2011;26:991–9.
[5] Klunk WE, Engler H, Nordberg A, Wang Y, Blomqvist G, Holt DP, et al. Imaging brain amyloid in Alzheimer's disease with Pittsburgh compound-B. Ann Neurol 2004;55:306–19.
[6] Storandt M, Mintun MA, Head D, Morris JC. Cognitive decline and brain volume loss as signatures of cerebral amyloid-beta peptide deposition identified with Pittsburgh compound B: cognitive decline associated with Abeta deposition. Arch Neurol 2009; 66:1476–81.
[7] Resnick SM, Sojkova J, Zhou Y, An Y, Ye W, Holt DP, et al. Longitudinal cognitive decline is associated with fibrillar amyloid-beta measured by [11C]PiB. Neurology 2010;74:807–15.
[8] Villemagne VL, Pike KE, Darby D, Maruff P, Savage G, Ng S, et al. Abeta deposits in older nondemented individuals with cognitive decline are indicative of preclinical Alzheimer's disease. Neuropsychologia 2008;46:1688–97.
[9] Pike KE, Savage G, Villemagne VL, Ng S, Moss SA, Maruff P, et al. Beta-amyloid imaging and memory in nondemented individuals: evidence for preclinical Alzheimer's disease. Brain 2007; 130:2837–44.
[10] Chetelat G, Villemagne VL, Pike KE, Ellis KA, Bourgeat P, Jones G, et al. Independent contribution of temporal beta-amyloid deposition to memory decline in the pre-dementia phase of Alzheimer's disease. Brain 2011;134:798–807.
[11] Morris JC, Roe CM, Grant EA, Head D, Storandt M, Goate AM, et al. Pittsburgh compound B imaging and prediction of progression from cognitive normality to symptomatic Alzheimer disease. Arch Neurol 2009;66:1469–75.
[12] Villemagne VL, Pike KE, Chetelat G, Ellis KA, Mulligan RS, Bourgeat P, et al. Longitudinal assessment of Abeta and cognition in aging and Alzheimer disease. Ann Neurol 2011;69:181–92.
[13] Aizenstein HJ, Nebes RD, Saxton JA, Price JC, Mathis CA, Tsopelas ND, et al. Frequent amyloid deposition without significant cognitive impairment among the elderly. Arch Neurol 2008; 65:1509–17.
[14] Oh H, Mormino EC, Madison C, Hayenga A, Smiljic A, Jagust WJ. Beta-amyloid affects frontal and posterior brain networks in normal aging. Neuroimage 2011;54:1887–95.
[15] Mormino EC, Kluth JT, Madison CM, Rabinovici GD, Baker SL, Miller BL, et al. Episodic memory loss is related to hippocampal-mediated beta-amyloid deposition in elderly subjects. Brain 2009; 132:1310–23.
[16] Landau SM, Harvey D, Madison CM, Koeppe RA, Reiman EM, Foster NL, et al. Associations between cognitive, functional, and FDG-PET measures of decline in AD and MCI. Neurobiol Aging 2011;32:1207–18.
[17] Landau SM, Harvey D, Madison CM, Reiman EM, Foster NL, Aisen PS, et al. Comparing predictors of conversion and decline in mild cognitive impairment. Neurology 2010;75:230–8.
[18] Jagust W, Gitcho A, Sun F, Kuczynski B, Mungas D, Haan M. Brain imaging evidence of preclinical Alzheimer's disease in normal aging. Ann Neurol 2006;59:673–81.
[19] de Leon MJ, Convit A, Wolf OT, Tarshish CY, DeSanti S, Rusinek H, et al. Prediction of cognitive decline in normal elderly subjects with 2-[(18)F]fluoro-2-deoxy-D-glucose/positron emission tomography (FDG/PET). Proc Natl Acad Sci U S A 2001;98:10966–71.
[20] Desikan RS, McEvoy LK, Thompson WK, Holland D, Roddey JC, Blennow K, et al. Amyloid-beta associated volume loss occurs only in the presence of phospho-tau. Ann Neurol 2011;70:657–61.
[21] Mungas D, Reed BR, Kramer JH. Psychometrically matched measures of global cognition, memory, and executive function for assessment of cognitive decline in older persons. Neuropsychology 2003;17:380–92.
[22] Squire LR, Zola SM. Episodic memory, semantic memory, and amnesia. Hippocampus 1998;8:205–11.
[23] Braak H, Braak E, Bohl J. Staging of Alzheimer-related cortical destruction. Eur Neurol 1993;33:403–8.

[24] Grober E, Hall CB, Lipton RB, Zonderman AB, Resnick SM, Kawas C. Memory impairment, executive dysfunction, and intellectual decline in preclinical Alzheimer's disease. J Int Neuropsychol Soc 2008;14:266–78.
[25] Amieva H, Carcaillon L, Rouze L'Alzit-Schuermans P, Millet X, Dartigues JF, Fabrigoule C. [Cued and uncued memory tests: norms in elderly adults from the 3 Cities epidemiological study]. Rev Neurol (Paris) 2007;163:205–21.
[26] Wechsler D. Wechsler Adult Intelligence Scale-III. San Antonio, TX: The Psychological Corporation; 1997.
[27] Price JC, Klunk WE, Lopresti BJ, Lu X, Hoge JA, Ziolko SK, et al. Kinetic modeling of amyloid binding in humans using PET imaging and Pittsburgh compound-B. J Cereb Blood Flow Metab 2005;25:1528–47.
[28] Fischl B, Salat DH, Busa E, Albert M, Dieterich M, Haselgrove C, et al. Whole brain segmentation: automated labeling of neuroanatomical structures in the human brain. Neuron 2002;33:341–55.
[29] Pike KE, Ellis KA, Villemagne VL, Good N, Chetelat G, Ames D, et al. Cognition and beta-amyloid in preclinical Alzheimer's disease: data from the AIBL study. Neuropsychologia 2011;49:2384–90.
[30] Mormino EC, Brandel MG, Madison CM, Rabinovici GD, Marks S, Baker SL, et al. Not quite PIB-positive, not quite PIB-negative: slight PIB elevations in elderly normal control subjects are biologically relevant. Neuroimage 2012;59:1152–60.
[31] Minoshima S, Frey KA, Foster NL, Kuhl DE. Preserved pontine glucose metabolism in Alzheimer disease: a reference region for functional brain image (PET) analysis. J Comput Assist Tomogr 1995;19:541–7.
[32] Desikan RS, Segonne F, Fischl B, Quinn BT, Dickerson BC, Blacker D, et al. An automated labeling system for subdividing the human cerebral cortex on MRI scans into gyral based regions of interest. Neuroimage 2006;31:968–80.
[33] Cohen J. Applied multiple regression/correlation analysis for the behavioral sciences. 3rd ed. Mahwah, NJ: L. Erlbaum Associates; 2003.
[34] Frazier PA, Tix AP, Barron KE. Testing moderator and mediator effects in counseling psychology research. J Couns Psychol 2004; 51:115–34.
[35] Field AP. Discovering statistics using SPSS: (and sex, drugs and rock' n' roll). 2nd ed. London: Sage Publications; 2005.
[36] Aiken LS, West SG. Multiple regression: testing and interpreting interactions. Newbury Park, CA: Sage Publications; 1991.
[37] Cohen J, Cohen P, West SG, Aiken LS. Applied multiple regression/correlation analysis for the behavioral sciences. 3rd ed. Mahwah, NJ: L. Erlbaum Associates; 2003.
[38] Cook RD, Weisberg S. Residuals and influence in regression. New York: Chapman and Hall; 1982.
[39] Rodrigue KM, Kennedy KM, Devous MD Sr, Rieck JR, Hebrank AC, Diaz-Arrastia R, et al. Beta-amyloid burden in healthy aging: regional distribution and cognitive consequences. Neurology 2012;78:387–95.
[40] Rowe CC, Ellis KA, Rimajova M, Bourgeat P, Pike KE, Jones G, et al. Amyloid imaging results from the Australian Imaging, Biomarkers and Lifestyle (AIBL) study of aging. Neurobiol Aging 2010; 31:1275–83.
[41] Jack CR Jr, Lowe VJ, Senjem ML, Weigand SD, Kemp BJ, Shiung MM, et al. 11C PiB and structural MRI provide complementary information in imaging of Alzheimer's disease and amnestic mild cognitive impairment. Brain 2008;131:665–80.
[42] Cohen AD, Price JC, Weissfeld LA, James J, Rosario BL, Bi W, et al. Basal cerebral metabolism may modulate the cognitive effects of Abeta in mild cognitive impairment: an example of brain reserve. J Neurosci 2009;29:14770–8.
[43] Rentz DM, Locascio JJ, Becker JA, Moran EK, Eng E, Buckner RL, et al. Cognition, reserve, and amyloid deposition in normal aging. Ann Neurol 2010;67:353–64.
[44] Goh JO, An Y, Resnick SM. Differential trajectories of age-related changes in components of executive and memory processes. Psychol Aging 2012;27:707–19.
[45] Drzezga A, Becker JA, Van Dijk KR, Sreenivasan A, Talukdar T, Sullivan C, et al. Neuronal dysfunction and disconnection of cortical hubs in nondemented subjects with elevated amyloid burden. Brain 2011;134:1635–46.
[46] Becker JA, Hedden T, Carmasin J, Maye J, Rentz DM, Putcha D, et al. Amyloid-beta associated cortical thinning in clinically normal elderly. Ann Neurol 2011;69:1032–42.
[47] Jack CR Jr, Knopman DS, Weigand SD, Wiste HJ, Vemuri P, Lowe V, et al. An operational approach to National Institute on Aging–Alzheimer's Association criteria for preclinical Alzheimer disease. Ann Neurol 2012;71:765–75.
[48] Jagust WJ, Mormino EC. Lifespan brain activity, beta-amyloid, and Alzheimer's disease. Trends Cogn Sci 2011;15:520–6.
[49] Desikan RS, McEvoy LK, Thompson WK, Holland D, Brewer JB, Aisen PS, et al. Amyloid-beta-associated clinical decline occurs only in the presence of elevated P-tau. Arch Neurol 2012;69:709–13.
[50] Sojkova J, Zhou Y, An Y, Kraut MA, Ferrucci L, Wong DF, et al. Longitudinal patterns of beta-amyloid deposition in nondemented older adults. Arch Neurol 2011;68:644–9.

Further Reading

[e1] Yesavage JA, Brink TL, Rose TL, Lum O, Huang V, Adey M, et al. Development and validation of a geriatric depression screening scale: a preliminary report. J Psychiatric Res 1982;17:37–49.
[e2] Folstein M, Folstein S, McHugh P. "Mini-mental state": a practical method for grading the cognitive state of patients for the clinicians. J Psychiatric Res 1975;12:189–98.
[e3] Delis DC, Kramer JH, Kaplan E, Ober BA. California Verbal Learning Test. 2nd ed. San Antonio, TX: Psychological Corporation; 2000.
[e4] Wechsler D. WMS-R: Wechsler Memory Scale–Revised: manual. San Antonio, TX: Psychological Corporation/Harcourt Brace Jovanovich; 1987.
[e5] Trenerry MR, Crosson B, DeBoe J, Leber WR. The Stroop Neuropsychological Screening Test. Odessa, FL: Neuropsychological Assessment Resources; 1989.
[e6] Benton AL, Hamsher KD. Multilingual aphasia examination. Iowa City, IA: AJA Associate; 1989.
[e7] Reitan RM. Validity of the trailmaking test as an indication of organic brain damage. Percept Mot Skills 1955;8:271–6.
[e8] Logan J, Fowler JS, Volkow ND, Wang GJ, Ding YS, Alexoff DL. Distribution volume ratios without blood sampling from graphical analysis of PET data. J Cereb Blood Flow Metab 1996;16:834–40.